Assessment of Aircraft Separation Reduction Potential for Arrivals Facilitated by Plate Lines

Dennis Vechtel[1]

German Aerospace Center (DLR), 38108 Braunschweig, Germany

Frank Holzäpfel[2] and Grigory Rotshteyn[3]

German Aerospace Center (DLR), 82234 Oberpfaffenhofen, Germany

Wake vortex related minimum aircraft separations for arrivals were evaluated utilizing plate lines. A plate line consists of a series of vertical plates placed in front of the runway that accelerate the decay of wake vortices. This study evaluates the potential to reduce minimum aircraft separations and the potential to increase safety due to the accelerated vortex decay. The presented method follows the methodology of the proposal for revised wake turbulence categorization RECAT-EU as much as possible in order to be compliant with the respective certified safety assessment. Wake vortex data measured by lidar with and without plates during a measurement campaign at Vienna International Airport, Austria, were used to generate generic non-dimensional decay curves for all captured aircraft types under so-called reasonable worst-case weather conditions with and without plates. The observed wake vortex behavior without plates was fitted to the generic decay curve from RECAT-EU. The application of the same method to the measurements with plates yields a generic decay curve representing the accelerated decay triggered by the plates. Applied to the RECAT-EU minimum separation scheme potential separation reductions ranging from 12% to 15% were evaluated. The same method was applied to the RECAT-EU-PWS pairwise separations, yielding a potential separation reduction due to the plates of 12% to 24% (average 14.8%) or a potential circulation reduction of about 20% to 30%. An assessment of the associated encounter risk showed significant benefits from plate lines indicating that the collaborative introduction of RECAT-EU-PWS together with plate lines may bring about increased airport capacity and safety at the same time when comparing it to the RECAT-EU scheme which is already operational at four European airports.

Nomenclature

α_1, α_2	=	decay coefficients (-)
Γ	=	vortex circulation (m²/s)
Γ_0	=	initial vortex circulation (m²/s)
Γ^*	=	normalized vortex circulation (-)
Λ	=	wing aspect ratio (-)
ρ	=	air density (kg/m³)
b	=	wing span (m)
b_0	=	initial vortex spacing (m)
g	=	gravitational acceleration (m/s²)
H	=	altitude (m)

---

[1] Research Engineer, Institute of Flight Systems, dennis.vechtel@dlr.de.
[2] Senior Scientist, Institute of Atmospheric Physics, Associate Fellow AIAA.
[3] Research Engineer, Institute of Atmospheric Physics.

m	=	mass (kg)
r_c	=	core radius (m)
t	=	time (s)
t_0	=	time scale (s)
t_d	=	onset time of the rapid decay (s)
t^*	=	normalized time (-)
V	=	airspeed (m/s)
$V_{app,min}$	=	minimum approach speed (m/s)
V_{stall}	=	stall speed (m/s)
w_0	=	initial vortex descent speed (m/s)

I. Introduction

Wake vortices from a preceding aircraft may pose a considerable threat to following aircraft. For this reason, minimum separation distances are defined to prevent trailing aircraft from hazardous wake encounters. The established wake-related aircraft separation schemes, such as e.g. from ICAO [1], have proven safe over the last decades. However, separation minima also limit airspace and airport capacities [2]. For this reason, a recategorization effort has been undertaken in recent years with the purpose to lower the minimum separations of those aircraft pairings that have shown to be overly conservative while maintaining the same level of safety. In Europe RECAT-EU [3] was established using six aircraft categories instead of the four categories introduced in the first place by ICAO.

The highest risk to encounter wake vortices of a preceding aircraft is during landing close to ground. An increase in encounter probability in ground proximity was shown by various simulations [4][5][6]. Those results are confirmed by an increased encounter occurrence close to ground documented by pilot reports [7][8][9]. In order to mitigate the risk of a wake encounter close to ground plate lines were investigated in recent years. A plate line consists of a number of vertical flat plates, placed parallel to each other and aligned with the flight direction installed in front of the runway at a distance of about 300 m to the touchdown zone (see Fig. 1).

Plate lines [10] trigger the early detachment of strong Ω-shaped secondary vortices that actively approach the wake vortices and subsequently propagate along the primary vortices. These secondary vortices lead to an accelerated wake vortex decay independent of natural external disturbances [11][12]. Lidar measurements confirm the functionality of the plate line [13] and flight simulator tests also showed a reduction of the encounter severity through the installation of plates [14]. Although the plates of course affect all vortices, the benefits of the plate line are most obvious if the most safety-relevant longest-living and strongest vortices are considered whose lifetime can be reduced by one third [13]. In potentially hazardous situations caused by persistent wake vortices that remain on the glide path of the approaching aircraft plate lines have shown to substantially reduce vortex lifetimes.

As the plate lines are very effective in accelerating the vortex decay, it is obvious to analyze the potential to further reduce minimum aircraft separations in case that plate lines are installed in front of a runway. In order to generate a large database of the influence of plate lines on the vortex decay a comprehensive lidar measurement campaign with and without plates was conducted at Vienna International Airport, Austria [15]. The measured vortex evolutions are the basis for the evaluation of a potential minimum separation reduction enabled by the installation of a plate line. In order to be compliant with the certified safety assessment of RECAT-EU (as an example of current minimum separation schemes), the approach follows the safety evaluation of RECAT-EU.

The RECAT-EU minimum separation scheme follows the approach of the ICAO minimum separation scheme to cluster aircraft in a few wake categories (ICAO: light, medium heavy, super). While ICAO only uses the maximum take-off weight MTOW as measure for the categorization, RECAT-EU uses the MTOW and the wing span as additional measure. Also, RECAT-EU introduces a few more wake categories (RECAT-EU: light, lower medium, upper medium, lower heavy, upper heavy, super) that allow for a separation reduction for many aircraft types in comparison to ICAO. In addition to RECAT-EU, RECAT-EU-PWS (pairwise separations) introduce a non-clustered, pairwise separation for each pair of aircraft types. RECAT-EU has been certified and is in operation at several airports. RECAT-EU-PWS is still under certification and not yet in operation.

Fig. 1 Plate line installed in front of runway 16 at Vienna International Airport, Austria (photo: DLR).

The method described here is designed to be as close as possible to the approach used in the RECAT-EU safety evaluation [3]. Nevertheless, some deviations from the RECAT-EU evaluation method could not be avoided, either because of some specific needs to deviate due to the characteristics of the plate lines (which are a deviation from RECAT-EU as such), or because of a lack of knowledge of some exact details of the RECAT-EU process. Intentional deviations from the RECAT-EU method are clearly marked and a justification for the deviation is given. The RECAT-EU method is largely adopted in order to suffice the requirements set forth by the approving authorities as close as possible.

The idea behind the method to evaluate possible benefits in minimum separations using plate lines in comparison to RECAT-EU is to generate generic dimensionless decay curves in analogy to RECAT-EU using lidar measurements with and without plates. First, the generic decay curve without plates is fitted to that from RECAT-EU. When the same method is applied to the measurements with plates, the resulting time shifts between the generic decay curves with and without plates are transferred into a difference in aircraft separation using aircraft specific approach speeds and masses.

II. Generation of a generic decay curve

Based on the lidar measurements of wake vortices accomplished at runway 16 of Vienna International Airport [15], a generic vortex circulation decay curve can be generated in analogy to the generic decay curve used in RECAT-EU. Generally, different generic decay curves can be generated using either measurements without plates or those with plates. By adapting the generic decay curve without plates to that from RECAT-EU, the accelerated vortex decay due to the plates can be referenced against RECAT-EU if an equivalent approach is applied to the measurements with plates.

A. Measurement dataset

The datasets from the Vienna measurement campaign include lidar measurements of vortices without plates and with plates. The lidars were scanning in five vertical planes perpendicular to the flight direction, located at a distance of 310 m, 400 m, 570 m, 740 m, and 910 m from the threshold of runway 16. Median flight altitudes above ground at the lidar planes L1 to L5 were determined from Mode-S data protocols to 39.9 m, 45.0 m, 53.6 m, 64.3 m, and 74.2 m, respectively, with a standard deviation of 4.2 m. The datasets comprise general data, such as date, time, the respective lidar scanning plane and aircraft type, as well as the specific measured values of the lateral and vertical vortex position, vortex age and circulation of each vortex measurement. The data include measurements of various aircraft types (A310, A320, A332, A333, A388, B744, B748, B752, B763, B772, B788, B789) with the A320, the B772 and the B763 being the aircraft types with the highest number of measurements. Hence, the most interesting RECAT-EU aircraft categories "upper heavy", "lower heavy" and "upper medium" are represented by at least one aircraft type with a statistically significant amount of data.

Although the evaluation as described in the following is performed for all aircraft by default (in order to be comparable to RECAT-EU), it is also possible to perform the evaluation for a specific aircraft type or aircraft category.

B. Data selection

The measurement data are subject to various selection criteria in order to ensure proper validity of the used data for further evaluation.

For A320 aircraft measurements from Lidar planes L4 and L5 are disregarded. As the vortex measurements following the RECAT-EU approach are intended to start at about one wing span above ground, these measurement planes with more than two wing spans height are excluded. For all other aircraft all Lidar planes are considered.

As the plate lines are designed to be only effective within a specific lateral safety corridor extending ±50 m in front of the runway [15], it is reasonable to disregard those vortices for the evaluation which are transported outside of this lateral corridor quickly by strong crosswind. Using those vortices for the evaluation would reduce the calculated plate benefits as vortices are considered which are not affected by the plates anymore (and hence decay more slowly). Also, those vortices are much less critical as the risk to encounter them is neglectable because a follower aircraft will fly within a relatively narrow lateral corridor before touch-down. For this reason, it is decided to disregard all vortices which leave the lateral safety corridor before a certain time unless they drift back into the corridor at any higher vortex age. Note that this criterion acts as a crosswind-filter, leaving cases with weak crosswind in the dataset.

Bourgois et al. [16] use a lateral safety corridor of ±100 m and disregard vortices which drift outside this corridor before 58 s. The value of 58 s corresponds to the minimum radar separation given typical approach speeds of transport aircraft. It is highly improbable that a following aircraft would encounter younger vortices than those with an age of 58 s. In order to be consistent with that quite reasonable criterion it is decided here to disregard vortices which drift outside the ±50 m corridor before a period of time of 29 s unless they drift back into the corridor at any higher vortex age.

Note that if a vortex is selected, always the full measured vortex evolution is considered. That means that no single measurements are disregarded in case they violate a criterion (e.g. outside the lateral corridor). If a vortex does not comply with a criterion, always the whole vortex evolution is disregarded.

C. Time shift

In order to allow a proper comparison between the vortices of different aircraft types, the considered vortex evolution shall always begin at a height of one wing span of the generator aircraft. As this cannot be guaranteed by the measurements, the vortex ages are shifted so that $t = 0$ is imposed always at a height of one generator's wing span.

This means in detail that each individual circulation decay curve is shifted in time such that the height of the vortices at $t = 0$ corresponds to the particular generator wing span. The required time shift Δt is calculated using the difference between the actual height of the first measurement h and the generator's wing span b and the initial vortex descent speed w_0.

$$\Delta t = \frac{\Delta H}{w_0} = \frac{(h-b)(2\pi b_0)}{\Gamma_0} \tag{1}$$

The initial circulation Γ_0 is estimated using the two-phase model fit described in the next section. The initial vortex spacing b_0 is estimated as an average from the measurements with and without plates for all recorded approaches of a specific aircraft type. Specifically, b_0 is evaluated as the median of the measured lateral spacings of port and starboard vortices over a period of time of $0.25 \cdot t_0$ (for calculation of t_0 see eq. (4)). As the determination of b_0 depends on t_0, this calculation needs to be performed iteratively. Figure 2 depicts the estimated initial vortex spacings $b_{0,estimate}$ for the different aircraft types in relation to the theoretical value of $b_{0,elliptic} = (\pi/4) \cdot b$ which is only valid for an elliptical lift distribution. The aircraft types A320, B763 and B772 are highlighted as they are used in the following for aircraft type specific evaluation.

4
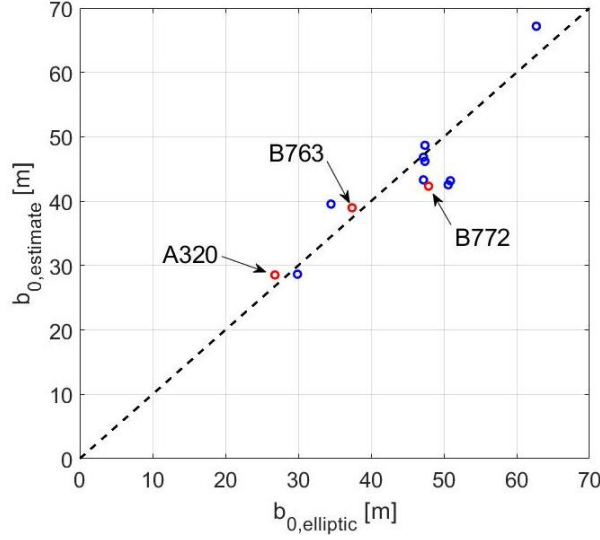
Fig. 2 Initial vortex spacings as evaluated from the measurements.

D. Two-phase decay model

For the further evaluation, the circulation measurements are not used directly but the vortex decay is modelled by a two-phase model [16]. The measured circulation evolutions are fitted by a two-phase decay model in order to smooth the data and to enable extrapolation to low circulation values. For the model fits the shifted time scale is used as described above. In ground proximity a phase of rapid decay typically is initiated following the initial gradual decay shortly after the vortices have reached the lowest altitude and start to rebound [17][18][19]. Out of ground effect also continuous decay or three-phased decay is observed depending on the environmental conditions [20][21].

The following equations [16] are used for the two decay phases differentiated by the time of the onset of the rapid decay t_d

$$\Gamma(t) = \begin{cases} \Gamma_0 \cdot e^{-\alpha_1 t} & for \ t \leq t_d \\ \Gamma_0 \cdot e^{(\alpha_2 - \alpha_1)t_d - \alpha_2 t} & for \ t > t_d \end{cases} \tag{2}$$

Each vortex considered as valid possesses a set of four fitted model parameters. The fitted parameters are the initial circulation Γ_0, the decay parameters α_1 and α_2 as well as the onset time of the rapid decay t_d. In order to reduce the computational effort, the range of Γ_0 was constrained by +/- 50 m²/s around the average circulation of the first three lidar measurements. No constraints are introduced for any of the other three fitting parameters.

The fitting is performed by minimizing the residues between the modelled circulation $\Gamma(\alpha_1, \alpha_2, t_d, \Gamma_0, t_i)$ and the measured circulation $\Gamma(t_i)$ via least-squares fits

$$res = \sum_{i=1}^{N} \big(\Gamma(\alpha_1, \alpha_2, t_d, \Gamma_0; t_i) - \Gamma(t_i) \big)^2 \tag{3}$$

For the further evaluation, as explained previously, only the modelled decay curves are used while the measurements are disregarded.

E. Generic decay curve

In order to generate a generic non-dimensional decay curve, all fitted model decay curves are normalized by the respective initial circulation Γ_0 and the time scale t_0 which is a function of the initial vortex spacing b_0 and the initial circulation Γ_0.

$$t_0 = 2\pi \frac{b_0^2}{\Gamma_0} \tag{4}$$

Here, the initial circulations from the model fits are used and not the measured ones.

Within RECAT-EU the longest-living vortices are considered for the generation of the generic decay curve for reasonable worst-case weather conditions, namely those whose lifetime is larger than $5.02 \cdot t_0$ [22]. The generic decay curve is the median of all those longest-living vortices. This approach is retained here for the measurements without

5

plates in order to be well aligned with the RECAT-EU approach. For the measurement data used in RECAT-EU this corresponds to 2% of all considered data [16]. Using the measurement data from the Vienna campaign together with the lifetime threshold used in the RECAT-EU process would lead to a different median decay curve. For this reason, the lifetime threshold was adapted here to $3.5 \cdot t_0$ in order to fit the generic decay curve with the Vienna measurements to that from RECAT-EU. The number of vortices reaching a lifetime of at least $3.5 \cdot t_0$ is 72.2% of all considered measurement data. The reason for this significantly larger percentage is that for the execution of measurements at Vienna airport and the selection of cases for processing preferably reasonable worst-case atmospheric conditions were considered, leading to a much longer lifetime of the vortices in average.

As the plate lines are designed to reduce the lifetime of the vortices, it is not meaningful to use the same vortex lifetime criterion with and without the plates. Instead the same percentage of longest-living vortices as without the plates (72.2% of all vortices) is selected to generate the corresponding reasonable worst-case decay curve with plate lines. This is justified because the measurement days and the processed vortex evolutions were chosen such that for both cases with and without plates similar ranges of headwind and crosswind speeds as well as thermal stratification and turbulence intensities were prevailing [23]. Using the same lifetime threshold with plates would lead to a much smaller fraction of valid vortices as the plate lines accelerate vortex decay for nominally identical environmental conditions.

The resulting generic decay curves from the medians of the selected longest-living vortices are depicted and compared to the RECAT-EU decay curve in Fig. 3.
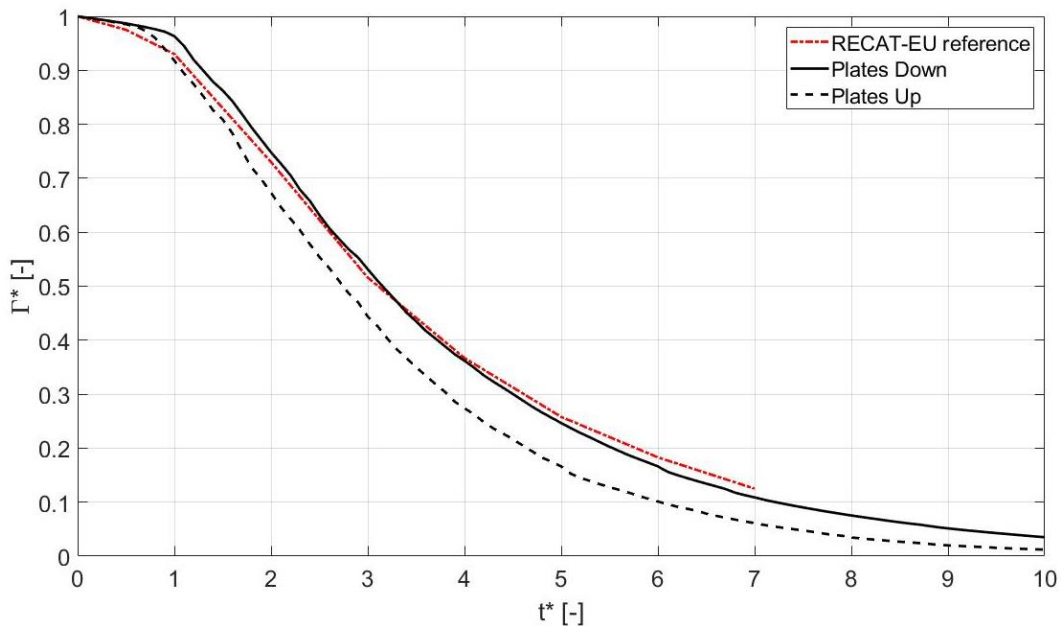
Fig. 3 Dimensionless decay curves with and without plates and RECAT-EU reference (all aircraft).

Figure 3 shows that the generic decay curve without plates matches that from RECAT-EU well. The two-phase decay characteristics are somewhat more pronounced for the decay curve based on the Vienna data. The good agreement of the decay curves of the different data sets provides good confidence that the applied methods are really equivalent. Further, it can be observed that the curve with plate lines is always below that without plates, representing the faster decay of the vortices induced by the plates.

For a better representation of the accelerated vortex decay Fig. 4 shows the difference of the dimensionless time shift Δt^* between the curves with and without plates as a function of the dimensionless vortex age, t^*. Obviously, the plate effect starts almost immediately after the generation of the vortices and leads to a relatively linearly increasing benefit over time.
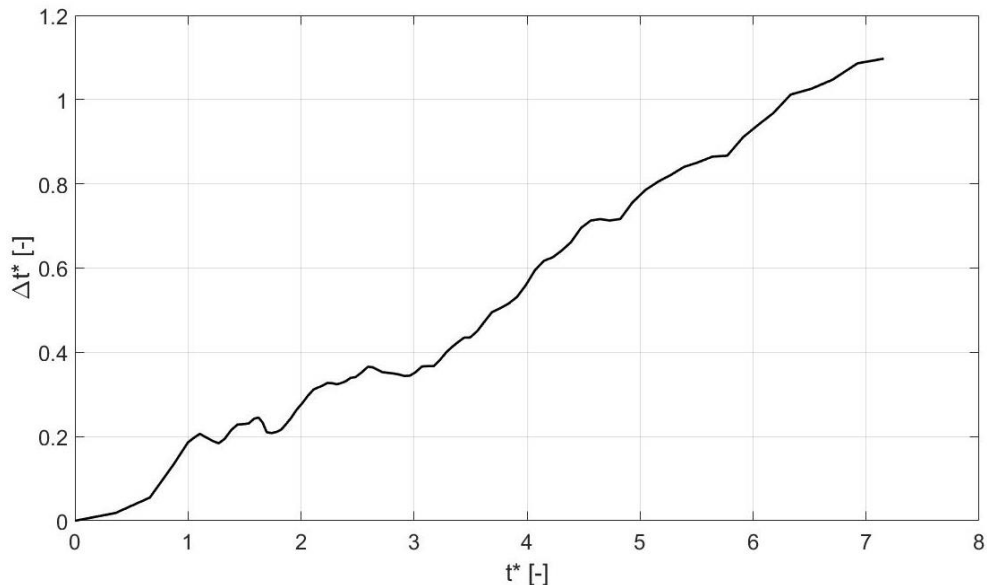
Fig. 4 Dimensionless time shift between the reasonable worst-case decay curves with and without plate lines (all aircraft).

F. Aircraft type-wise evaluation

As on one hand the lidar dataset is dominated by the medium weight class A320 and on the other hand the plates effectiveness is more pronounced for heavy aircraft [15], it is interesting to perform the evaluation not only for all aircraft but for specific aircraft types as well.

For the aircraft type-wise evaluation the same threshold for the selection of the longest-lived vortices is applied, namely, that the vortex lifetime is longer than $3.5 \cdot t_0$. However, this results in a different percentage of the selected vortices. These amount for the B772 to 74.3%, for the B763 to 83.3% and for the A320 to 70.7%. Figure 5 to Figure 7 show the generic decay curves of those three aircraft types in comparison to the generic decay curve from RECAT-EU.
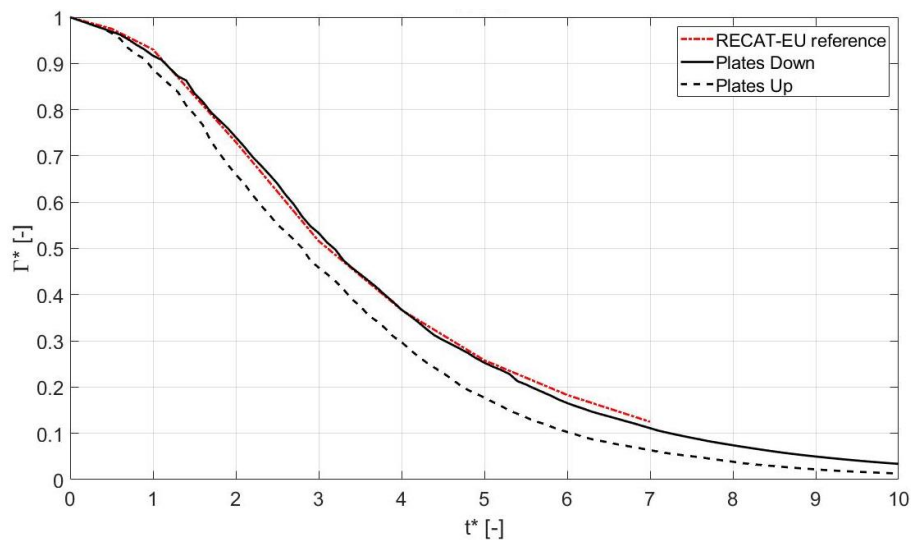
Fig. 5 Dimensionless decay curves with and without plates and RECAT-EU reference (A320 only).
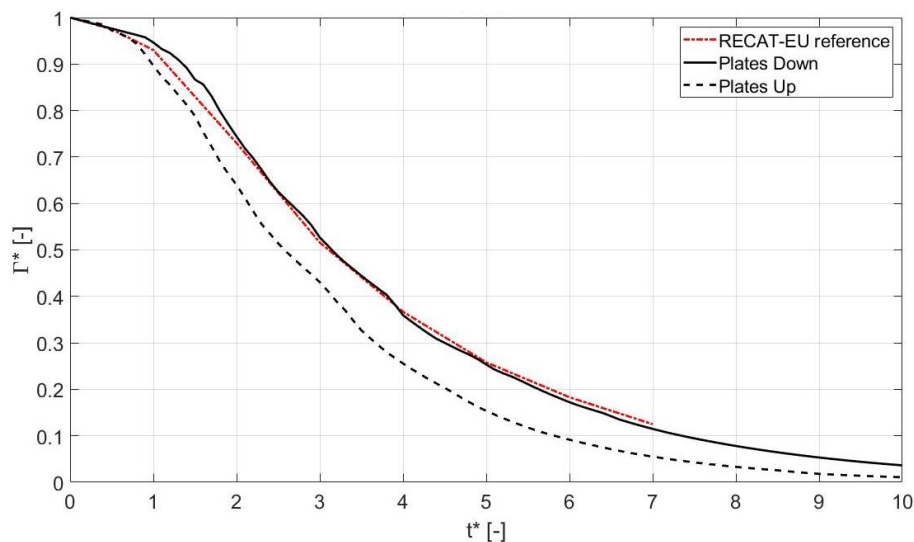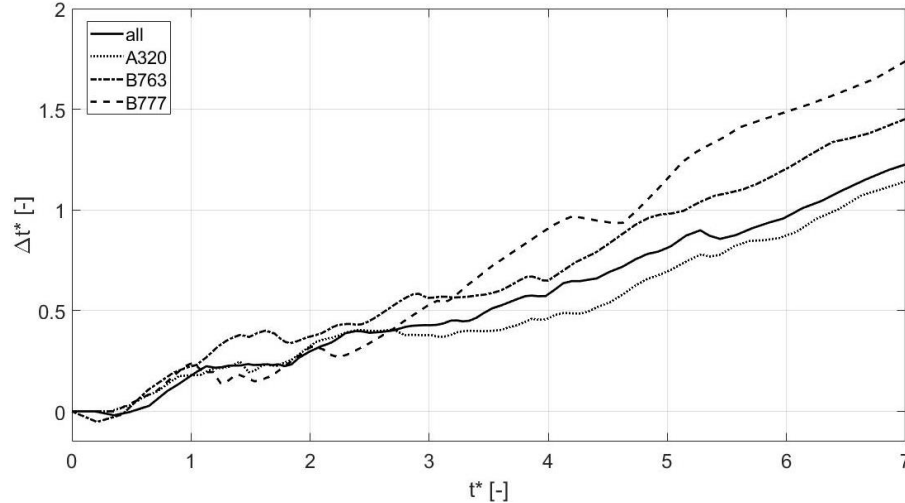
Fig. 6 Dimensionless decay curves with and without plates and RECAT-EU reference (B763 only).
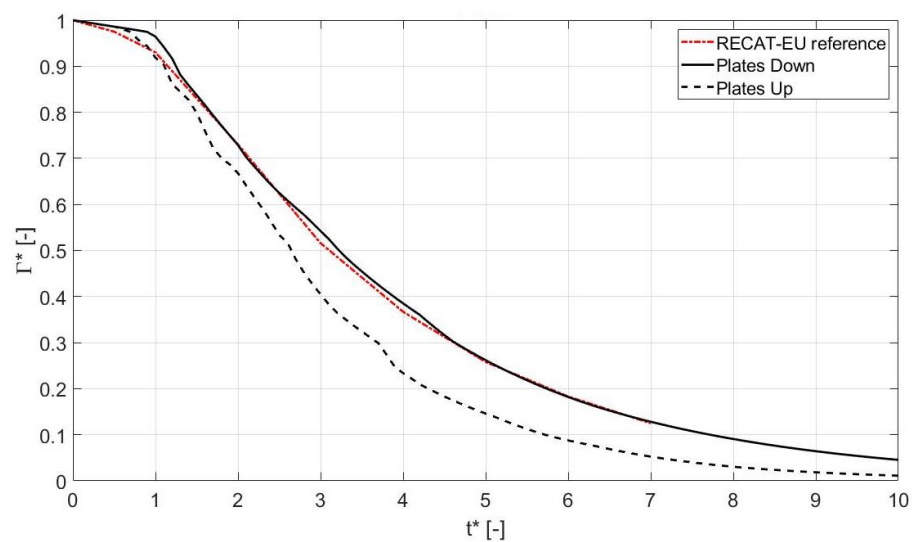
Fig. 7 Dimensionless decay curves with and without plates and RECAT-EU reference (B772 only).

The aircraft type specific decay curves show without exception that it is possible to fit the decay curve without plates to that from RECAT-EU using all vortex evolutions with vortex ages beyond $3.5 \cdot t_0$. However, the significantly smaller overall number of vortex evolutions of B763 and B772 result in less smoother curves than for the A320.

The resulting differences in dimensionless time for the three example aircraft types are outlined in Figure 8 together with the curve for all aircraft shown in Figure 4.

Fig. 8 Dimensionless time differences between the generic decay curves with and without plates for specific aircraft types.

Figure 8 shows that for higher vortex ages ($t^* > 3$) the plate benefit is more pronounced for the heavier aircraft. Also, the domination of the data by the A320 contributing 74% of the vortices can be observed. Up to a vortex age of about $t^* = 3$ the curve for all aircraft follows closely the curve of the A320 evaluation. For vortex ages greater than $t^* = 3$ the increased benefit of the heavy aircraft lifts the curve of all aircraft, but it still remains distinctly below that of the B772 and B763.

As the A320 as wake generator aircraft is only relevant for light aircraft in the minimum separation scheme, the potential benefit from the plate effect is underestimated when using all aircraft types for the generic decay curve weighted by the number of eligible lidar measurement data. An increase of the fraction of measurements of heavy aircraft in the database would very probably lead to a further increased benefit for higher vortex ages. This should be considered for future lidar measurement campaigns.

III.   Evaluation of benefits for the RECAT-EU minimum separation scheme

Based on the generic decay curve described in the previous chapter revised minimum separations can be evaluated which assure that the maximum circulation that a follower aircraft might be exposed to is not larger than under adherence to the RECAT-EU minimum separations. At least this is true in that part of the final approach which is considered most critical, because there wake vortices may rebound to the flight paths.

A. Representative aircraft used for evaluation

As the generic decay curve without plates equals the generic decay curve from RECAT-EU it can act as reference regarding minimum aircraft separations for approach and landing. Given the approach speed of an aircraft the separation distance as prescribed by RECAT-EU can be translated into a separation time, or vortex age, respectively. This means that under adherence to the RECAT-EU minimum separations a following aircraft can be exposed to a specific maximum circulation which is regarded as safe, as demonstrated by the RECAT-EU safety case [3]. Consequentially, it can be expected that if a following aircraft is exposed to the same circulation at an earlier vortex age with plates, this must be safe as well. Therefore, this vortex age with plates can be retranslated into a separation distance.

Note that the RECAT-EU safety case postulates "the follower aircraft encounters the wake vortex while flying close to the ground during its approach to landing. It is acknowledged that reportable wake turbulence encounters can also occur on the glide slope and especially at glide slope intercept during approach operations. Due to the missing interaction with the ground boundary layer the vortex strength is typically larger for identical separation distances under these circumstances. Nevertheless, these operational scenarios are regarded as less hazardous compared to encounters close to ground because more height above ground remains for counteracting the adverse effects of an encounter." [3] Whether or not this rationale still can be applied with the reduced vortex lifetimes in ground proximity facilitated by plate lines is not within the scope of this investigation and has to be demonstrated elsewhere.

For the evaluation of minimum separation distances following the method described above, the generic dimensionless decay curve needs to be made dimensional using specific aircraft data of the leader / generator aircraft.

9

For the translation of separation distances into separation times also specific aircraft data of the follower aircraft are required. Altogether, for the leader aircraft the true airspeed, the mass and the wing span are required for the estimation of Γ_0 and b_0; while for the follower aircraft the true airspeed is required for the translation of separation distances to temporal separations and vice versa.

For the evaluation of revised minimum separation distances using plate lines 82 aircraft types are considered, which represent most of the air traffic worldwide. These aircraft types are listed in Table 1.

Table 1 Aircraft types used for the evaluation based on RECAT-EU separations.

Super Heavy	Upper Heavy	Lower Heavy	Upper Medium	Lower Medium	Light
A388	A332 B77W	A306 L101	A318 T204	AN32 CRJ2	BE40 P180
A124	A333 B788	A30B MD11	A319	AT43 CRJ9	C525 SF34
	A342 IL96	A310	A320	AT45 DC93	C650
	A343	B703	A321	AT72 DH8D	D328
	A345	B752	AN12	B462 E135	E120
	A346	B753	B736	B712 E145	FA10
	A359	B762	B737	B732 E170	FA20
	B744	B763	B738	B733 E190	H25B
	B748	B764	B739	B734 F70	JS32
	B772	DC10	C130	B735 F100	JS41
	B773	DC85	MD82	CL60 RJ85	LJ35
	B77L	IL76	MD83	CRJ1 RJ1H	LJ60

As each of the 82 aircraft types in Table 1 can act as leader and as follower, the true airspeed, wing span and mass are required for all these aircraft types. The wing span is a fixed value and available for all considered aircraft. The other two parameters are generally variable and may differ from source to source. For this reason, representative values for the approach speed and a typical aircraft mass during approach are required for each aircraft type. Unfortunately, the values used in RECAT-EU are not available publicly. Therefore, reasonable values for the approach speed and the aircraft mass during approach are estimated here. In order to evaluate the sensitivity of those parameters a variation within a meaningful range is performed.

The approach speed is estimated based on the stall speed given in the BADA database [24]. The minimum approach speed is $V_{app,min} = 1.3 \cdot V_{stall}$. In order to evaluate the sensitivity of the approach speed, the evaluation is also performed with a 20 kts higher approach speed. Even with the 20 kts increase in the approach speed the maximum resulting separation changes are only in the order of magnitude of about 0.1 NM. Specifically, the change in minimum separation is only noticeable for heavies behind heavies. For all other pairings the change due to the increase of approach speed is below 0.1 NM.

The aircraft mass during approach is estimated to be 85% of the maximum landing weight (MLW) as found in measurements conducted at the airports Memphis and Dallas Fort Worth [25]. Another method to estimate the landing weight of aircraft is given in [26]. However, for reasons of simplicity the value of 85% MLW is used here. In order to evaluate the sensitivity of the parameter the aircraft mass is varied between 50% MLW and 100% MLW. For the variation of the aircraft mass the change is only noticeable for heavies behind heavies as well. Again, for all other pairings the change is below 0.1 NM. From this minor sensitivity of separation distances to the required aircraft parameters one may conclude that the use of aircraft data employed for the RECAT-EU method would most likely lead to almost identical results.

From the parameters described above the initial circulation Γ_0 (eq. 5) and the time scale t_0 (eq. 4) are evaluated

$$\Gamma_0 = \frac{mg}{\rho b_0 V} \tag{5}$$

where for the air density the value of the International Standard Atmosphere at sea level of $\rho = 1{,}225$ kg/m³ is used. For both parameters the initial vortex spacing b_0 is required. As actual values for b_0 are only available for the aircraft types from the measurements and not for all 82 aircraft from Table 1, the theoretical value for an elliptic lift distribution with the wing span b is used here for all aircraft types

$$b_0 = \frac{\pi}{4} b \tag{6}$$

Using Γ_0 and t_0 for each generator aircraft, the generic decay curves (with and without plates) are made dimensional. For each follower aircraft the RECAT-EU minimum separation distance is transferred into a temporal separation using the approach speed of the follower. For this time (vortex age) the circulation Γ is evaluated from the dimensional decay curve without plates, which equals the RECAT-EU reference curve. For this circulation the respective vortex age of the decay curve with plates is evaluated. This vortex age is translated back into separation distance using the follower aircraft's approach speed. This method is exemplarily illustrated in Figure 9 with B773 as leader and SF34 as follower.
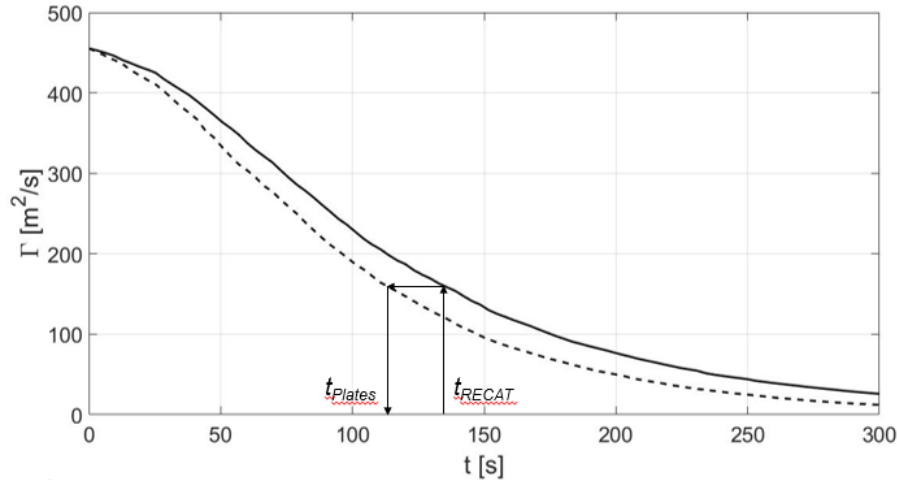
Fig. 9 Exemplary illustration of the evaluation of aircraft type specific minimum separation distances.

B. Separation Reduction Potential

Following the approach described above a minimum separation can be evaluated for each pair of the 82 aircraft, yielding an 82 x 82 matrix of separation distances for the considered aircraft pairings. These minimum separations are then grouped into the aircraft categories as defined in RECAT-EU. In order to be conservative, the minimum separations with plates are the maxima of all pairwise separations for the respective category (e.g. the minimum separation with plates for "lower medium" behind "upper heavy" is the maximum of all "lower mediums" behind all "upper heavies").

Table 2 outlines the evaluated separation minima with plates in nautical miles for each aircraft category as defined in RECAT-EU. The numbers below the minimum separations are the differences to the respective RECAT-EU minimum separations as absolute values (in NM) and as percentages. The aircraft separation reduction potential varies between 12% and 15% depending on the aircraft categories.

11

Table 2 Separation matrix with plate lines and difference to RECAT-EU (absolute and relative).

Leader / Follower		Super Heavy	Upper Heavy	Lower Heavy	Upper Medium	Lower Medium	Light
		A	B	C	D	E	F
Super Heavy	A	**2.6 NM** -0.4 NM -13.3 %	**3.4 NM** -0.6 NM -15.0 %	**4.4 NM** -0.6 NM -12.0 %	**4.4 NM** -0.6 NM -12.0 %	**5.2 NM** -0.8 NM -13.3 %	**6.9 NM** -1.1 NM -13.8 %
Upper Heavy (B772)	B		**2.6 NM** -0.4 NM -13.3 %	**3.5 NM** -0.5 NM -12.5 %	**3.5 NM** -0.5 NM -12.5 %	**4.4 NM** -0.6 NM -12.0 %	**6.0 NM** -1.0 NM -14.3 %
Lower Heavy (B763)	C			**2.6 NM** -0.4 NM -13.3 %	**2.6 NM** -0.4 NM -13.3 %	**3.5 NM** -0.5 NM -12.5 %	**5.2 NM** -0.8 NM -13.3 %
Upper Medium (A320)	D						**4.3 NM** -0.7 NM -14.0 %
Lower Medium	E						**3.4 NM** -0.6 NM -15.0 %
Light	F						**2.6 NM** -0.4 NM -13.3

As outlined in section II.F. the benefit of the plates is bigger for heavier leading aircraft. In order to evaluate the possible additional benefit if the lidar database would not be dominated as much by the medium aircraft A320 as it is the case here, the separations are evaluated in a second step using the generic decay curves from B772 (representing the upper heavies), B763 (representing the lower heavies) and A320 (representing the upper mediums). Of course, not the full separation matrix can be evaluated this way, but only for the three aforementioned leader aircraft categories. Table 3 depicts the results for these three leader aircraft.

Table 3 Separation matrix with plates and difference to RECAT-EU (absolute and relative) using the generic decay curves for B772, B763 and A320 as leaders.

Leader / Follower		Super Heavy	Upper Heavy	Lower Heavy	Upper Medium	Lower Medium	Light
		A	B	C	D	E	F
B772	B		**2.4 NM** -0.6 NM -20.0 %	**3.3 NM** -0.7 NM -17.5 %	**3.3 NM** -0.7 NM -17.5 %	**4.1 NM** -0.9 NM -18.0 %	**5.3 NM** -1.7 NM -24.3 %
B763	C			**2.6 NM** -0.4 NM -13.3 %	**2.6 NM** -0.4 NM -13.3 %	**3.4 NM** -0.6 NM -15.0 %	**5.1 NM** -0.9 NM -15.0 %
A320	D						**4.5 NM** -0.5 NM -11.1 %

Using leader-specific decay curves the aircraft separation reduction potential varies in a larger range between 10% and 20% depending on the aircraft categories. It can be observed in Table 3 that the separation benefit is especially pronounced for lower medium and light aircraft behind the B772. For the B763 the increase of the plate benefit is even more pronounced. Altogether, the changes compared to the baseline evaluation using all aircraft reflects the aircraft-specific changes to the baseline already observed in Figure 8. This is also the reason why the A320 shows a smaller benefit using only A320 measurements.

IV. Evaluation of benefits for the RECAT-EU-PWS minimum separation scheme

In analogy to the evaluation for the RECAT-EU minimum separations an assessment was performed for the benefits of plate lines concerning the pairwise minimum separations of RECAT-EU-PWS [27]. Here, the generic decay curve from section II was applied again.

### A. Representative aircraft used for evaluation

In the RECAT-EU-PWS safety case report [27] a slightly different set of representative aircraft is used compared to the RECAT-EU safety case report [3]. In order to be as close as possible to the original assessment of RECAT-EU-PWS a slightly different set of aircraft is used for the evaluation presented here as well. Table 4 outlines the aircraft types used for the evaluation of benefits from the use of plate lines for RECAT-EU-PWS. One can easily observe in comparison to Table 1 that the most prominent aircraft types are used here as well. Altogether, the aircraft types shown in Table 4 represent 96.41% of the arrival traffic based on CFMU traffic data recorded between August 2014 and September 2014 covering the top 25 ECAC airports [27]. In comparison to the assessment for RECAT-EU separations in section III (see Table 1), here the amount of aircraft of the lower medium and light category is increased. This makes sense, as those aircraft are especially vulnerable to wake encounters behind heavy leaders. Therefore, it is reasonable to focus more on those aircraft types when designing pairwise separations.

Table 4 Aircraft types used for the evaluation based on RECAT-EU-PWS separations (aircraft type index for plotting in parenthesis).

Super (S)	Upper Heavy (UH)	Lower Heavy (LH)	Upper Medium (UM)	Lower Medium (LM)		Light (L)	
A388 (1)	B748 (2)	MD11 (16)	B739 (25)	A148 (35)	F27 (51)	SF34 (66)	C25A (82)
	B77L (3)	B764 (17)	B738 (26)	B734 (36)	F50 (52)	D328 (67)	C525 (83)
	B77W (4)	B762 (18)	B737 (27)	B733 (37)	DH8D (53)	E120 (68)	C510 (84)
	A359 (5)	B763 (19)	B736 (28)	B735 (38)	AT75 (54)	C680 (69)	P46T (85)
	B744 (6)	A306 (20)	A321 (29)	E190 (39)	AT72 (55)	C56X (70)	PA34 (86)
	A346 (7)	A30B (21)	A320 (30)	GL5T (40)	FA7X (56)	C25C (71)	
	A345 (8)	A310 (22)	A318 (31)	GLEX (41)	AT43 (57)	LJ45 (72)	
	B773 (9)	B752 (23)	A319 (32)	GLF5 (42)	AT45 (58)	H25B (73)	
	B772 (10)	B753 (24)	MD83 (33)	B712 (43)	CRJ2 (59)	C560 (74)	
	A343 (11)		MD82 (34)	F100 (44)	E145 (60)	LJ60 (75)	
	A332 (12)			F70 (45)	E135 (61)	BE40 (76)	
	A333 (13)			B463 (46)	F2TH (62)	LJ35 (77)	
	A342 (14)			RJ1H (47)	F900 (63)	B350 (78)	
	B788 (15)			RJ85 (48)	FA50 (64)	C25B (79)	
				E170 (49)	CL60 (65)	PC12 (80)	
				CRJ9 (50)		C550 (81)	

B. Separation Reduction Potential

Applying the same methodology as described in section III. the potential for reduction of minimum separations is evaluated for the RECAT-EU-PWS separations. Figure 10 depict the absolute and relative separation reduction potential for the 86 aircraft types shown in Table 4. The aircraft types are depicted only by their index as outlined in Table 4 as a labeling with the exact name would be barely readable. Low numbers indicate heavy aircraft and high numbers indicate light aircraft. However, in order to give a better overview, the boundaries of the RECAT-EU aircraft categories are shown by the dashed lines.

13
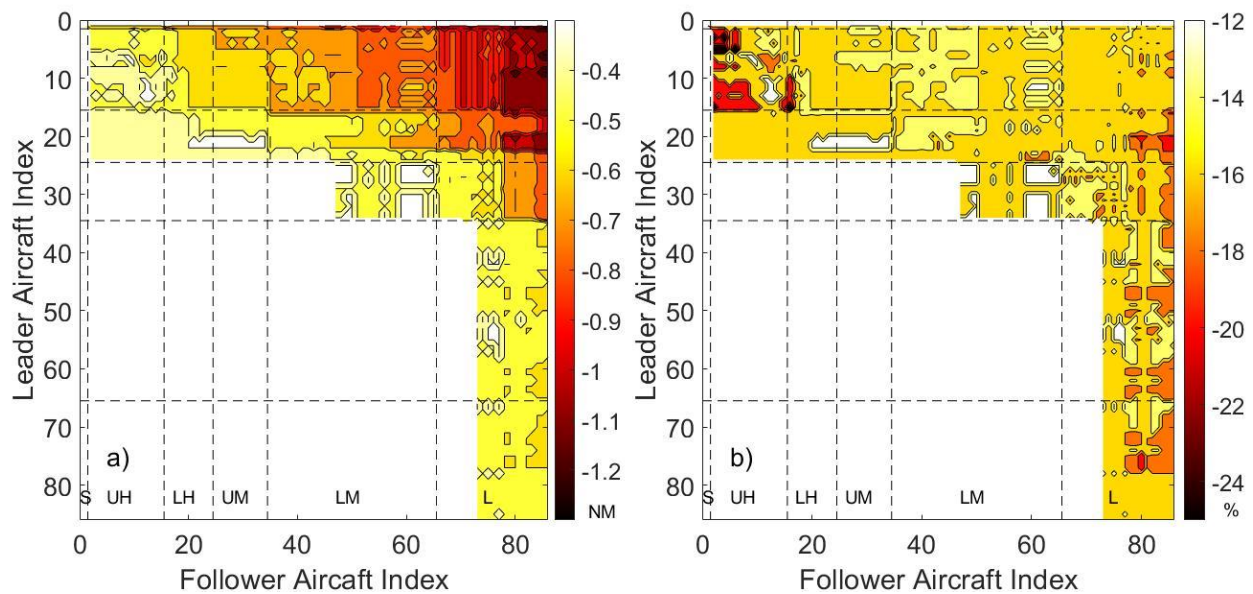
Fig. 10   Separation reduction potential with plates for RECAT-EU-PWS separation minima – a) absolute in NM, b) relative in percent).

Figure 10 shows an absolute reduction potential of circa 0.4 NM to 1.3 NM, which corresponds to approximately 12% to 24%. The average over all aircraft pairings is 14.8%. Hence, the reduction potential shown here is in the order of magnitude of the reduction potential evaluated for RECAT-EU (Table 2) and even higher for some aircraft pairings. That the reduction potential evaluated for pairwise separations is higher for some pairs compared to a category-based approach such as RECAT-EU is reasonable as the clustering of aircraft into categories always leads to over-conservativism for single aircraft pairs. One can clearly observe in Fig. 10a that the largest absolute gain is for the light aircraft behind heavy leaders. This can be explained by the increasing plate effect with increasing vortex age. The relative gain shown in Fig. 10b shows a wide region of aircraft pairings with a benefit close to the average of 15%. This means that the relative benefit is similar for most aircraft pairings. The only aircraft pairs with larger relative benefits are some of the heaviest followers behind upper heavy leaders and some light followers behind leaders of different categories. The first ones can be explained by the already very low separation distance, for which even a small absolute gain is already a large percental gain. The latter ones can be explained again by the large vortex age for light followers, hence the larger plate effect connected to it.

C. Circulation Reduction Potential at RECAT-EU-PWS separations

The effect of the plates to accelerate the vortex decay could also be used to lower the severity of a possible wake encounter without changing the minimum aircraft separations. As already shown in Fig. 9 the vortex circulation with plates lies below that without plates for a given vortex age. A given separation distance corresponds to a specific vortex age and therefore to a circulation for a given leader aircraft. The plate effect can therefore be expressed through a reduction of circulation by comparing the decay curves with and without plate lines.

Figure 11 shows the circulation reduction for the RECAT-EU-PWS separation minima. The left-hand side of Fig. 11 shows the circulation reduction related to the respective circulation at the vortex age corresponding to the specific RECAT-EU-PWS separation distance. The right-hand side of Fig. 11 shows the circulation reduction related to the respective initial circulation of the leader aircraft Γ_0. Again, the boundaries of the RECAT-EU aircraft categories are depicted by dashed lines to give a better overview on the aircraft types.

14
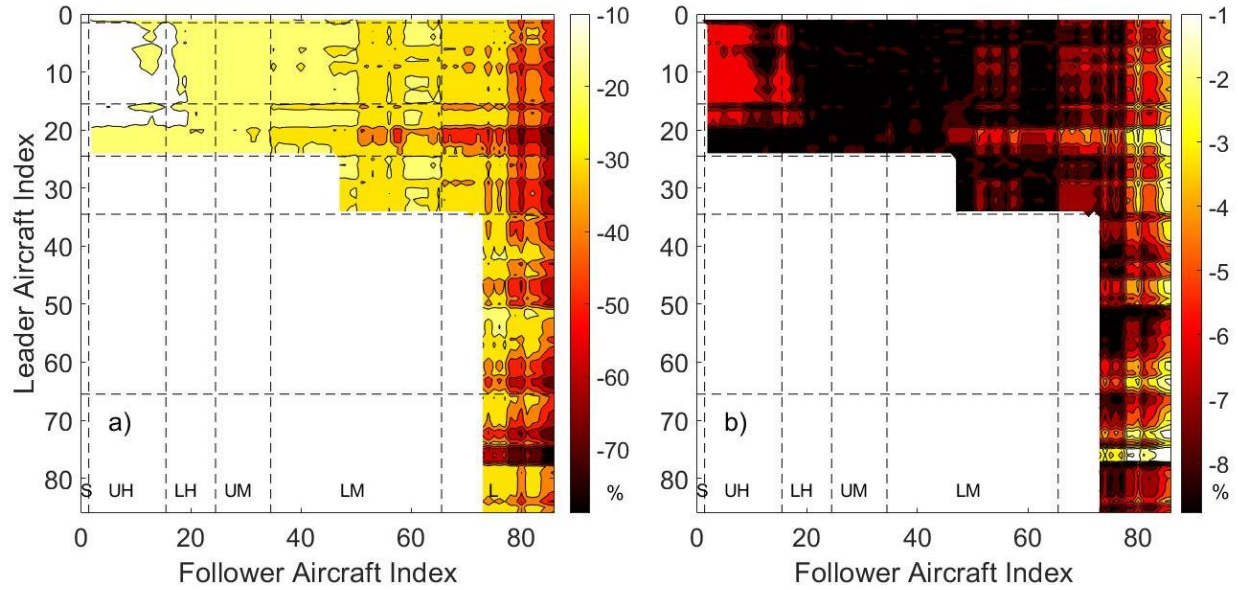
Fig. 11 **Circulation reduction in percent with plates for RECAT-EU-PWS separation minima - a) related to** Γ **(**$t_{RECAT\text{-}EU\text{-}PWS}$**), b) related to** Γ_0**.**

The left side of Fig. 11 shows for some aircraft pairs a maximum circulation reduction of more than 70% of the circulation at the respective vortex age. However, these extreme values only apply for some aircraft pairings, whereas for the majority of aircraft pairs especially in the heavy and medium categories the benefit is around 20-30%. The right side of Fig. 11 shows that the circulation reduction related to the leader's initial circulation is about 6-8% for a variety of aircraft pairs. The comparison of the left- and right-hand side of Fig. 11 reveals that those aircraft pairs with the largest reductions in the left plot show the least reductions in the right plot. This might sound counterintuitive at first. However, all of those aircraft pairs with extremely large reductions if related to the circulation at vortex age and very low reductions if related to the initial circulation feature separation distances corresponding to large vortex ages. At those ages the vortices are already almost decayed. The very low circulation level at those vortex ages allows for very large percental reductions by the plates, whereas the absolute circulation reduction is marginal. Those cases should not be over-rated. The main conclusion is that Fig. 11a shows a wide area of aircraft pairs with a sound circulation reduction potential of up to 30%, which could be directly used as a safety gain.

As shown in the next section, the reduction of circulation can be translated into a risk reduction as it reduces the severity of possible wake encounters.

V. Risk Assessment

The risk of an event is known as the severity of the event times the frequency of its occurrence. For a wake encounter the severity can be expressed by the rolling moment coefficient (*RMC*) of the induced rolling moment. Here, the same equation for the *RMC* as in the RECAT-EU-PWS safety case report is used [27][28].

$$RMC = \frac{\Gamma(t_{age})}{V_f b_f} \frac{\Lambda_f}{\Lambda_f + 4} \left(1 - 2\left(2\frac{r_c}{b_l}\frac{b_l}{b_f}\right)\left(\sqrt{1 + \left(2\frac{r_c}{b_l}\frac{b_l}{b_f}\right)^2} - \left(2\frac{r_c}{b_l}\frac{b_l}{b_f}\right)\right)\right) \tag{7}$$

As can be seen the equation for the *RMC* only depends on the circulation at the vortex age corresponding to the respective aircraft separation $\Gamma(t_{age})$, the follower's airspeed V_f as well as some geometrical parameters of the leader and follower aircraft, namely the follower's aspect ratio Λ_f, the follower's wing span b_f and the vortex core radius normalized by the leader's wing span $r_c/b_l = 0.035$ [27]. In order to determine $\Gamma(t_{age})$ from the normalized reasonable worst-case decay curve (see Fig. 3), the vortex time scale t_0 according to eq. (4) and the initial circulation Γ_0 according to eq. (5) are employed. So, the *RMC* also depends on air density but more importantly on the initial vortex separation b_0 here approximated as $\pi/4$ times the wingspan assuming elliptical circulation distribution. As the assumed b_0 values

enter the vortex time scale t_0 cubed, *RMC* estimates based on measured b_0 values may deviate substantially from the estimates taken here.

In the RECAT-EU-PWS safety case report the traffic mix of the top 25 ECAC airports recorded between August and September 2014 is used to evaluate the frequency of occurrence of the *RMC* values needed for the risk assessment. It is assumed that each aircraft pairing results in an encounter at minimum separation, so that the fraction of the aircraft types within the traffic mix can be used as frequency of occurrence. Of course, in reality the rate of occurrence of an encounter is significantly lower, because it is highly unlikely that an aircraft may encounter the wake vortex core and most vortices are anyway transported away from the flight track of a follower aircraft. For this reason and because the *RMC* is calculated using the reasonable worst-case decay curve, the risk will be significantly smaller in reality. The risk assessment as presented here can be regarded as the absolute worst case.

With the *RMC* and the rate of occurrence of each aircraft pairing the Complementary Cumulative (probability) Distribution Functions (CCDF) of the pairwise *RMC* values are calculated for the separation schemes of ICAO, RECAT-EU and RECAT-EU-PWS.

Using the follower's airspeed being $V_{app,min} = 1.3 \cdot V_{stall}$ and an aircraft mass of 85% MLW (see section III.A.) the B748 yields the highest *RMC*, hence is the worst-case leader. In the RECAT-EU-PWS safety case assessment the A346 turned out to be the worst-case leader. This difference stems from the more elaborate airspeeds, aircraft masses, and initial vortex separations used in the RECAT-EU-PWS safety case, which were not available for the assessment presented here. Note that the B748 wing design features a pronounced root loading leading to lower values of vortex spacing b_0 and consequently faster circulation decay [29]. Here we assume elliptical circulation distribution for all aircraft types. However, the exact fit of *RMC* leading to the exact same worst-case leaders is considered of minor significance as long as the same method is used for each aircraft so that a relative assessment between cases with and without plate lines is still valid. Nevertheless, the different values for mass, initial vortex spacing and airspeed of each aircraft inevitably result in discernibly different CCDF curves compared to the RECAT-EU-PWS assessment.

In order to evaluate the robustness of the approach against parameter changes the percental amount on the traffic mix of the B748, being the worst-case leader, is varied. Figure 12 shows that the variation of the amount of the worst-case leader leads to significantly different ends of the CCDF curves at high RMC, which are especially crucial.
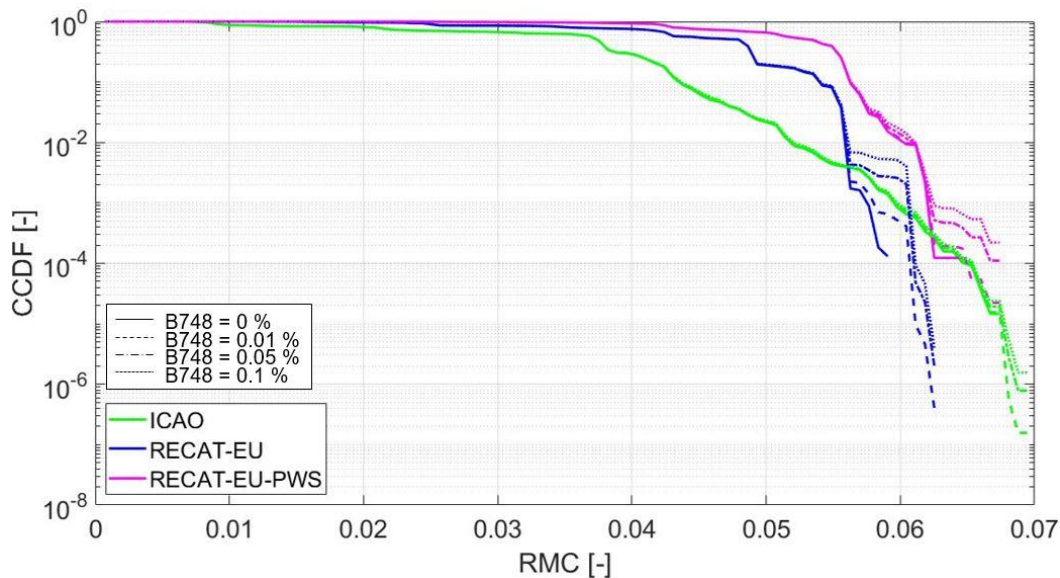
Fig. 12   Sensitivity of CCDF with variation of percental amount of B748 on traffic mix (all aircraft behind heavy leaders).

That the method is sensitive to the amount of the traffic share of the worst-case aircraft indicates that the risk assessment depends on the selected traffic mix. In order to increase the robustness of the safety considerations of pairwise separations against changes in the traffic mix and the selected aircraft parameters landing mass, approach speed and initial vortex separation, plate lines commend themselves as an effective means, as shown very clearly in Fig. 13.

16
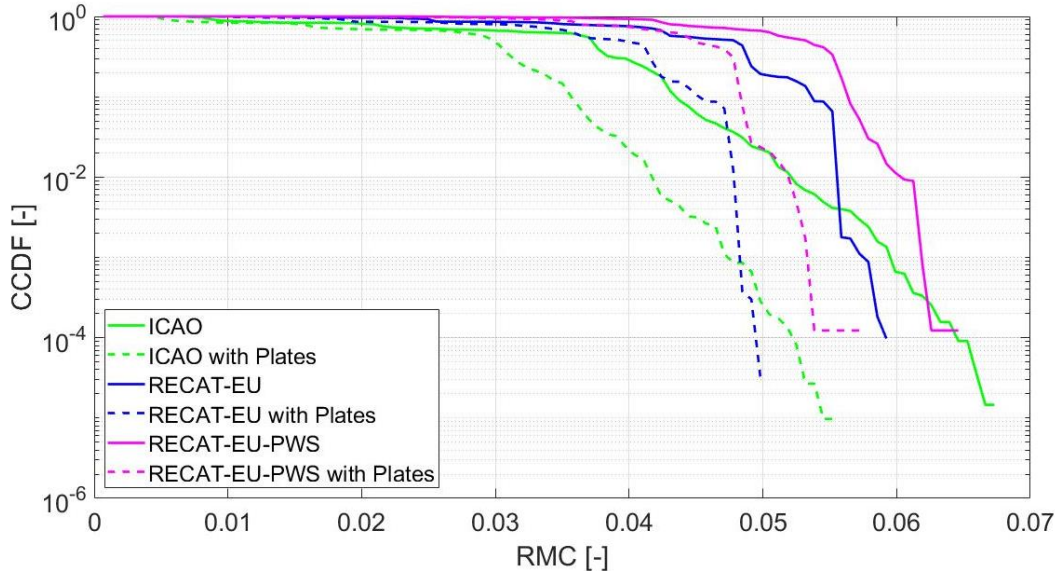
Fig. 13   CCDF for ICAO, RECAT-EU and RECAT-EU-PWS separations with and without plates (all aircraft behind heavy leaders).

Fig. 13 depicts the CCDF of the ICAO, RECAT-EU and RECAT-EU-PWS separation scheme with and without plates. One can easily observe the strong effect of the plates in mitigating the risk. With plates the CCDF of RECAT-EU-PWS lies even significantly below the CCDF of RECAT-EU without plates (and the CCDF of RECAT-EU with plates lies for the major part of the curve below that of ICAO without plates). Even though the exact values of some parameters used here differ from those used in the RECAT-EU or RECAT-EU-PWS safety cases, the large effect of the plates that can be observed in Fig. 13 gives good confidence that the plates are able to counteract the increased risk from lowered aircraft separations even if the traffic mix may change in the future. So, the introduction of the RECAT-EU-PWS scheme in combination with plate lines at a busy airport may increase both, the runway throughput for arrivals and the safety in terms of the wake vortex encounter risks compared to the RECAT-EU scheme which is successfully operational at four European airports (Paris Charles de Gaulle, London-Heathrow, Leipzig/Halle, and Toulouse).

VI.   Conclusion

The aim of the investigation described in this paper was to evaluate the potential to reduce the minimum aircraft separations for approach and landing using plate lines that accelerate wake vortex decay during final approach in ground proximity.

The method described here uses the generic circulation decay curve for reasonable worst-case weather conditions from RECAT-EU as reference. By fitting the almost identically generated decay curve from the Vienna lidar measurements without plates to the generic decay curve of RECAT-EU a certified reference is used that is accepted to be sufficiently safe.

The applied method guarantees that the circulation to which a follower aircraft may be exposed to during final approach under reasonable worst-case conditions when applying the revised minimum separations with plates is not higher than under adherence to the RECAT-EU or RECAT-EU-PWS minimum separations, respectively. Hence, the reduced separations should have the same level of safety as RECAT-EU or RECAT-EU-PWS, respectively. However, this is only true for those regions of the final approach where the plates accelerate the vortex decay, namely at very low altitude close to the runway. This region is considered the most critical as in ground effect the vortices may rebound to the flight corridor and therefore increase the encounter risk in particular for long-living wake vortices occurring under atmospheric conditions with low wind and minor turbulence. Nevertheless, a concluding answer whether the reduced encounter risk in ground proximity due to the plates can motivate a further reduction of minimum aircraft separations also along the glidepath could not be given, yet. This will be subject to future work on the benefit of plates for dynamic pairwise separations.

It was shown that using plate lines the minimum separations could potentially be reduced by about 13% to 16% for the different RECAT-EU aircraft categories and in average by about 15% for RECAT-EU-PWS pairwise

separations. It was also shown that without any change in the minimum separations the vortex circulation at the corresponding vortex age can be reduced by 20% to 30% for most aircraft pairs.

In addition, it was presented that the effect of the plate lines is more pronounced for heavier wake vortex generators. As the dataset of lidar measurements at Vienna airport is dominated by the A320, it can be expected that the potential benefit from the plates could even be further increased if only measurements from the respective aircraft category were considered (e.g. only upper heavies for the evaluation of separations with upper heavies as leader). However, in order to use all available measurement data for maximum statistical significance, the evaluation of minimum separations is performed using measurements from all aircraft types in the dataset.

With a risk assessment employing the rolling moment coefficient *RMC* to characterize encounter severity and the traffic mix from the top 25 ECAC airports to characterize the frequency of occurrence, the risk of the separation schemes under worst-case conditions was investigated following the method employed for the RECAT safety cases. It was found that the installation of plate lines could substantially reduce wake vortex encounter risks for all three considered separation schemes (ICAO, RECAT-EU, RECAT-EU-PWS), bringing the encounter risk of RECAT-EU-PWS down to a risk level even below that of RECAT-EU (and that of RECAT-EU for the greater part down below that of ICAO).

The possibly most attractive scenario constitutes the introduction of the RECAT-EU-PWS scheme together with the installation of plate lines which may improve both, the runway throughput for arrivals and the safety in terms of the wake vortex encounter risks compared to the RECAT-EU scheme which is successfully operational at four European airports since several years.

Acknowledgments

References

[1]   Procedures for Air Navigation Services – Rules of the Air and Air Traffic Services, Doc 4444-RAC/501. ICAO, 2006.

[2]   Donohue, G. L., and Rutishauer, L., "The Effect of Aircraft Wake Vortex Separation on Air Transportation Capacity", 4th FAA/Eurocontrol R&D Conference, Santa Fe, New Mexico, USA, December 2001.

[3]   N.N., "European Proposal for revised Wake Turbulence Categorisation and Separation Minima on Approach and Departure "RECAT – EU" Safety Case Report", Edition 2.0, EUROCONTROL, Brussels, Belgium, 2017, 234 pages.

[4]   Holzäpfel, F., et al., "Aircraft wake vortex scenarios simulation package – WakeScene," Aerospace Science and Technology, Vol. 13, no. 1, 2009, pp. 1-11. doi: 10.1016/j.ast.2007.09.008.

[5]   Kauertz, S., "Wake Vortex Encounter Risk Assessment using High-Fidelity Flight Simulation," German Aerospace Congress, DLRK-1301, Hamburg, Germany, 31 August - 2 September 2010.

[6]   Speijker, L.J.P., Kos, J., Blom, H.A.P., and van Baren, G.B., "Probabilistic Wake Vortex Safety Assessment to Evaluate Separation Distances for ATM Operations," 22nd International Congress of the International Council of the Aeronautical Sciences, Harrogate, UK, 27 August – 1 September 2000.

[7]   N. N., "Flight Safety Digest – Data Show That US. Wake-turbulence Accidents Are Most Frequent at Low Altitude and During Approach and Landing," Flight Safety Foundation, Vol. 21, no. 3-4, 2002.

[8]   Critchley, J.B., and Foot, P.B., "United Kingdom Civil Aviation Authority Wake Vortex Database: Analysis of Incidents Reports Between 1982 and 1990," Civil Aviation Authority, CAA Paper 91015, London, UK, 1991.

[9]   Holzäpfel, F., "Analysis of potential wake vortex encounters at a major European airport," Aircraft Engineering and Aerospace Technology, Vol. 89, no. 5, 2017, pp. 634-643. doi: 10.1108/AEAT-01-2017-0043.

[10] Stephan, A., Holzäpfel, F., and Misaka, T., "Hybrid simulation of wake-vortex evolution during landing on flat terrain and with plate line," International Journal of Heat and Fluid Flow, Vol. 49, 2014, pp. 18-27. doi: 10.1016/j.ijheatfluidflow.2014.05.004.

[11] Doligalski, T.L., Smith, C.R., and Walker, J.D.A., "Vortex Interactions with Walls," Annual Review of Fluid Mechanics, Vol. 26, 1994, pp. 573–616. doi: 10.1146/annurev.fl.26.010194.003041.

[12] Stephan, A., Holzäpfel, F., and Misaka, T., "Aircraft Wake-Vortex Decay in Ground Proximity - Physical Mechanisms and Artificial Enhancement," Journal of Aircraft, Vol. 50, no. 4, 2013, pp. 1250-1260. doi: 10.2514/1.C032179.

[13] Holzäpfel, F., Stephan, A., Heel, T., and Körner, S., "Enhanced Wake Vortex Decay in Ground Proximity Triggered by Plate Lines," Aircraft Engineering and Aerospace Technology, Vol. 88, no. 2, 2016, pp. 206-214. doi: 10.1108/AEAT-02-2015-0045.

[14] Vechtel, D., Stephan, A., Holzäpfel, F., "How Plate Lines Influence the Hazard Perception of Pilots During Wake Encounters", Journal of Aircraft, Vol. 57, 2020, pp. 360-367, https://doi.org/10.2514/1.C035689.

[15] Holzäpfel, F., Stephan, A., Rotshteyn, G., Körner, S., Wildmann, N., Oswald, L., Gerz, T., Borek, G., Floh, A., Kern, C., Kerschbaum, M., Nossal, R., Schwarzenbacher, J., Strobel, M., Strauss, L., Weiß, C., Kauczok, S., Schiefer, C., Czekala, H., Maschwitz, G., Smalikho, I., "Mitigating Wake Turbulence Risk During Final Approach via Plate Lines," AIAA Journal, Article in Advance, published 10 August 2021, https://doi.org/10.2514/1.J060025.

[16] Bourgeois, N., Choroba, P. and Winckelmans, G., Conditional reduction of ICAO wake turbulence separation minima on final approach, 5th International Conference on Research in Air Transportation, 22-25 May 2012, University of Berkeley, CA, USA.

[17] Proctor, F. H., Hamilton, D. W., and Han, J., "Wake Vortex Transport and Decay in Ground Effect: Vortex Linking with the Ground," AIAA Paper No. 2000-0757, Jan. 2000.

[18] Holzäpfel, F., and Steen, M., "Aircraft Wake-Vortex Evolution in Ground Proximity: Analysis and Parameterization, *AIAA* Journal, Vol. 45, No. 1, 2007, pp. 218-227.

[19] Holzäpfel, F., Tchipev, N., Stephan, A.,"Wind Impact on Single Vortices and Counterrotating Vortex Pairs in Ground Proximity", Flow, Turbulence and Combustion, Vol. 97, 2016, pp. 829–848, http://dx.doi.org/10.1007/s10494-016-9729-2.

[20] Proctor, F.H., Ahmad, N.N., Switzer, G.S., Limon Duparcmeur, F.M., "Three-Phased Wake Vortex Decay," AIAA Paper 2010-7991, 2010, 11 pages.

[21] Holzäpfel, F., Misaka, T., Hennemann, I., "Wake-Vortex Topology, Circulation, and Turbulent Exchange Processes," AIAA Paper 2010-7992, 2010, 16 pages.

[22] De Visscher, I. and Winckelmans, G., Characterization of Aircraft Wake Vortex Circulation Decay in Reasonable Worst Case Conditions, AIAA 2016-1603, 54th AIAA Aerospace Sciences Meeting, 4-8 January 2016, San Diego, CA, USA.

[23] Holzäpfel, F., Vechtel, D., Rotshteyn, G., Stephan, A., "Aircraft Separation Reduction Potential for Arrivals Facilitated by Plate Lines," submitted for publication to Flow.

[24] N.N., Base of Aircraft Data (BADA) Revision 3.13, May 2015, Eurocontrol, Brussels, Belgium.

[25] Delisi, D.P., et al., Estimates of the Initial Vortex Separation Distance, b_0, of Commercial Aircraft from Pulsed Lidar Data, AIAA 2013-0365, 51st AIAA Aerospace Sciences Meeting, 7-10 January 2013, Grapevine, TX, USA.

[26] Holzäpfel, F., Rotshteyn, G., "Estimating Aircraft Landing Weights from Mode S Data," 2022 AIAA SciTech Forum, 3–7 January 2022, San Diego, CA, 8 pages, also submitted to J. Aircraft.

[27] N.N., Wake Turbulence Re-Categorisation and Pair-Wise Separation Minima on Approach and Departure "RECAT-EU-PWS" Safety Case Report, Edition 2.0, EUROCONTROL, Brussels, Belgium, 2021.

[28] De Visscher et al., A Simple and Usable Wake Vortex Encounter Severity Metric, WakeNet-Europe Workshop 2015, Amsterdam, The Netherlands, 21-22 April 2015.

[29] Crouch, J. D., Czech, M. J., "Comparative Wake Wake-Turbulence Assessments and Findings for the B747-8," 4th WakeNet3-Europe Workshop, Feb. 2012, http://www.wakenet.eu/fileadmin/user_upload/4th_major_WN3E-Workshop/presentations/WN3E_2_01_Crouch_WV%2012%20WakeNet3Europe_Feb12_B747-8.pdf